ACS OMEGA

Article

http://pubs.acs.org/journal/acsodf

Biodegradable and Bioactive PCL–PGS Core–Shell Fibers for Tissue Engineering

Lijuan Hou,[†,‡] Xing Zhang,[‡] Paiyz E. Mikael,[*,‡] Lei Lin,[‡] Wenjun Dong,[†,∥] Yingying Zheng,[†] Trevor John Simmons,[‡,§] Fuming Zhang,[‡] and Robert J. Linhardt[*,‡]

[†]Center for Nanoscience and Nanotechnology, Zhejiang Sci-Tech University, 5 Second Avenue, Xiasha Higher Education Zone, Hangzhou 310018, P. R. China

[‡]Center for Biotechnology and Interdisciplinary Studies and [§]The Center for Future Energy Systems, Rensselaer Polytechnic Institute, 110 Eighth Street, Troy, New York 12180, United States

[∥]School of Materials Science and Engineering, University of Science and Technology Beijing, 30 Xueyuan Road, Haidian District, Beijing 100083, P. R. China

S *Supporting Information*

ABSTRACT: Poly(glycerol sebacate) (PGS) has increasingly become a desirable biomaterial due to its elastic mechanical properties, biodegradability, and biocompatibility. Here, we report microfibrous core–shell mats of polycaprolactone (PCL)–PGS prepared using wet–wet coaxial electrospinning. The anticoagulant heparin was immobilized onto the surface of these electrospun fiber mats, and they were evaluated for their chemical, mechanical, and biological properties. The core–shell structure of PCL–PGS provided tunable degradation and mechanical properties. The slowly degrading PCL provided structural integrity, and the fast degrading PGS component increased fiber elasticity. Young's modulus of PCL–PGS ranged from 5.6 to 15.7 MPa. The ultimate tensile stress ranged from 2.0 to 2.9 MPa, and these fibers showed elongation from 290 to 900%. The addition of PGS and grafting of heparin improved the attachment and proliferation of human umbilical vein endothelial cells. Core–shell PCL–PGS fibers demonstrate improved performance as three-dimensional fibrous mats for potential tissue-engineering applications.

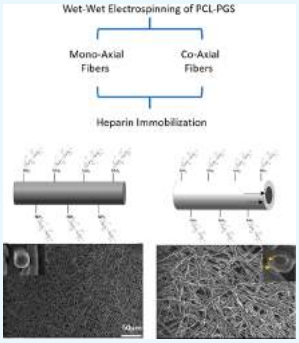

INTRODUCTION

The engineering of biomimetic three-dimensional scaffolds requires the precise design of tissue-engineering elements beyond the physical space where cells can attach, proliferate, and migrate. Engineered scaffolds should have adequate mechanical properties to withstand the forces acting on a tissue or an organ; thus, the choice of materials, processing methods, and chemical structure play a major role. The materials used must also be biocompatible to avoid an adverse immunological reaction and to facilitate seamless progression of healing and regeneration. Biodegradability and its rate are also essential design components. The ideal scaffold should degrade at a rate similar to the healing rate of the tissue or organ.[1−4]

Electrospinning has been used extensively for various biomedical applications. Synthetic, natural polymers, and their blends have been used in electrospinning, wherein fibers are spun into woven or nonwoven three-dimensional scaffolds. Electrospinning allows for a controlled design of the fiber size from micro to nanofibers, fiber alignment, control of pore size and porosity, and the use of monofilament and coaxial fiber structures, with the encapsulation of various agents (cells, growth factors, small molecules, nanoparticles, etc.). Post-electrospinning modification of fibers relying on fiber surface chemistry allows for immobilization and further functionalization of electrospun scaffolds to promote tissue regeneration and repair.[5−10] Both wet–dry and wet–wet electrospinning techniques can be implemented. Wet–dry electrospinning relies on a volatile solvent that evaporates during the electrospinning process, leaving dry polymeric fibers at the collecting plate, whereas in wet–wet electrospinning, the fibers are collected in a coagulation bath that is miscible with the spinning solvent but does not dissolve the polymer. Wet–wet electrospinning also permits the use of nonvolatile solvents in the electrospinning process.[11,12]

Poly(glycerol sebacate) (PGS) was initially designed for soft tissue engineering due to this polymers' excellent recovery from deformation.[13−17] PGS is a synthetic biocompatible elastomer that can be easily synthesized from glycerol and sebacic acid and degrades by surface erosion.[13,18,19] However, PGS prepolymer has low viscosity, and thus an additional chemical or physical process is needed to cure this polymer into solid materials. In one study, acrylated PGS was used with PEO followed by cross-linking,[20] whereas another study used thermal curing of PGS and poly(L-lactic acid) (PLLA) blends to prepare core–shell nanofibers.[21] Polycaprolactone (PCL) is a semicrystalline and aliphatic polyester that degrades slowly in

Received: April 14, 2017
Accepted: July 19, 2017
Published: October 2, 2017

DOI: 10.1021/acsomega.7b00460
ACS Omega 2017, 2, 6321−6328

vivo by either chemical hydrolysis of its ester bonds to caproic acid and its oligomers or through enzymatic hydrolyosis.[22−24] The high tensile strength, good elongation properties, excellent biocompatibility, and ease of chemical and physical modification has made PCL useful for a wide range of biomedical applications.[23,25] PCL and PGS have been combined as blends and as core−shell microfibers. Elastomeric microfibers of nonacrylated PGS were fabricated using wet−dry electrospinning by blending with PCL to increase the viscosity of PGS.[26] This study demonstrated that the addition of PGS to PCL improved the utility of microfibers for the growth of human umbilical vein endothelial cells (HUVECs). Recently, Masoumi et al.[27] fabricated aligned PGS/PCL microfibers to induce human aortic VIC's proliferation and maturation. Moreover, a study combining electrospinning with soft lithography was used to fabricate PGS/PCL electrospun patterned fibers to mimic the complex anisotropic and multiscale architecture of a cardiac tissue.[27]

In this study, for the first time, core−shell fiber mats of PCL−PGS were prepared using wet−wet coaxial electrospinning without chemically or physically curing PGS.

Heparin, a widely used polysaccharide-based anticoagulant drug, was immobilized on the surface of the resulting PCL−PGS mats.[28,29] We hypothesized that wet−wet coaxial electrospinning would facilitate the fabrication of PCL−PGS microfibers and that the resulting core−shell fibers would provide structural properties that resembled those of a natural extracellular matrix of a wide range of tissues and organs, depending on the PCL−PGS combination used. Heparin was also used to enhance surface properties of PCL−PGS mats and thus allow better cell adhesion, proliferation, and migration. The core−shell structure should also allow the encapsulation of cells, growth factors, and small molecules to guide the regeneration process.

MATERIALS AND METHODS

Materials. PGS prepolymer was synthesized on the basis of previous reports' processes.[27,30] Briefly, 1:1 molar ratio of sebacic acid and glycerol were reacted at 120 °C under high vacuum (≈50 mTorr) for 24 h. Polycaprolactone (PCL, MW 80 000), 2,2,2-trifluoroethanol (TFE), hexamethylenediamine, 1-ethyl-3-(3-dimethyl amino propyl) carbodiimide (EDC), *N*-hydroxy succinimide (NHS), tributylamine, and isopropanol were obtained from Sigma-Aldrich (St. Louis, Missouri). Human umbilical vein endothelial cells (HUVECs), endothelial basal medium-2 (EBM-2), and bullet kit were purchased from Lonza (MD). Lyophilized United States Pharmacopeia (USP) heparin from porcine intestinal mucosa was obtained from Celsus Laboratories Inc (Cincinnati, OH). Heparan sulfate (HS) disaccharide standards (Table S1 in the Supporting Information (SI)) were purchased from Iduron (Manchester, U.K.). High-performance liquid chromatography grade ammonium acetate, calcium chloride, acetic acid, and acetonitrile were purchased from Fisher Scientific (Springfield, New Jersey). *Escherichia coli* expression and purification of the recombinant *Flavobacterium heparinum* heparin lyase I−III (Enzyme Commission (EC) #s 4.2.2.7, 4.2.2.X, 4.2.2.8) were performed in our laboratory, as previously described. BIOPHEN Heparin Anti-IIa and Anti-Xa kits were purchased from ANIARA Diagnostica (West Chester, OH).

Fabrication of PCL−PGS Mats. PCL−PGS core−shell solutions were prepared by dissolving 13% (w/v) PCL in the TFE solution as the shell solution and 0, 40, 60, 80% (w/v) PGS in TFE as the core solution. The shell and core solutions were then mechanically stirred using a magnetic stirrer at room temperature to form homogeneous solutions. The core−shell fibers were fabricated, as previously described,[31] using a coelectrospinning process with a coaxial spinneret (MECC, Ogori, Fukuoka, Japan). The diameter of the inner needle and outer needle were 0.94 and 2.50 mm, respectively. The distance between the spinneret tip and aluminum collector electrode was fixed at 15 cm. The flow rates of the shell and core solutions were 180 and 30 μL/min, respectively. After electrospinning core−shell fibers, the weight percent (wt %) of 13% PCL−0% PGS (w/v) core−shell fiber was 100%, 13% PCL−40% PGS (w/v) was 66.1% PCL and 33.9% PGS, 13% PCL−60% PGS (w/v) was 56.5% PCL and 43.5% PGS, and 13% PCL−80% PGS (w/v) was 49.4% PCL and 50.6% PGS. The PCL−PGS mixture solutions were used as controls. Mixture fibers were prepared by dissolving 13% (w/v) PCL in a TFE solution and mechanically stirred using a magnetic stirrer at room temperature to form homogeneous solutions. The corresponding weight percent (wt %) of PGS was then added into the PCL solution, as in core−shell fibers (0, 40, 60, and 80%). The mixture solution of PCL and PGS was placed into a 10 mL syringe and connected to the spinneret (MECC, Ogori, Fukuoka, Japan). The internal diameter of the needle was 0.94 mm. The distance between the spinneret tip and the aluminum collector electrode was fixed at 15 cm. The electrospinning solution was fed at 30 μL/min. The scaffolds were marked with 13PCL, 13PCL−m-40PGS, 13PCL−m-60PGS, and 13PCL−m-80PGS, respectively. The applied voltage for both core−shell and mixture fibers was optimized at 15 kV. All electrospun fibers were collected into a water coagulation bath to remove TFE, washed with water, and freeze-dried under vacuum.

Fiber Mat Characterization. For morphological evolution of fiber mats, a field emission scanning electron microscope (FE-SEM) (FEI−Versa, Hillsboro) was used. For SEM observation, the samples were sputter-coated by a thin layer of gold and palladium. Prior to cross-sectioning, the mats were immersed in liquid nitrogen. The presence of PCL and PGS was confirmed by a Bruker D8-discover X-ray diffractometer using graphite-monochromated Cu Kα radiation. Thermal properties of PGS−PCL scaffolds were determined using a differential scanning calorimeter (DSC) 8500 (Perkin-Elmer). Preweighted scaffolds were sealed in aluminum pans and were heated at 10 °C min^{-1}. The samples were then subjected to six heating and cooling cycles between −80 and 100 °C under nitrogen condition. The presence of heparin was confirmed by its enzymatic digestion, followed by disaccharide analysis using liquid chromatography−mass spectrometry (LC−MS) (Agilent 6300 Ion Trap LC/MS Systems; CA). The LC separation was achieved using an Agilent Poroshell 120, EC-C18 column, (2.1 mm × 100 mm, 2.7 mm) at 55 °C on the Agilent 1200 LC system. The full-scan (200−900 Da) MS analysis was under negative ionization mode, with a skimmer voltage of −40.0 V, a capillary exit of −40.0 V, and a source temperature of 350 °C. Liquid nitrogen was used as the drying and nebulizing gas at a flow rate of 8 L/min and a pressure of 40 psi, respectively. Data analysis was performed using Agilent ChemSolution software.

Mechanical Properties. For mechanical measurements of the electrospun mats, a uniaxial elongation test was performed using an Instron 5800 (Plansee, Franklin, MA) load frame with a 100 N load cell. Specimens were cut to a rectangular shape (15 mm × 5 mm × 0.3 mm, n = 3); the crosshead speed was set constant at 10 mm/min during the uniaxial test. Young's

DOI: 10.1021/acsomega.7b00460
ACS Omega 2017, 2, 6321−6328

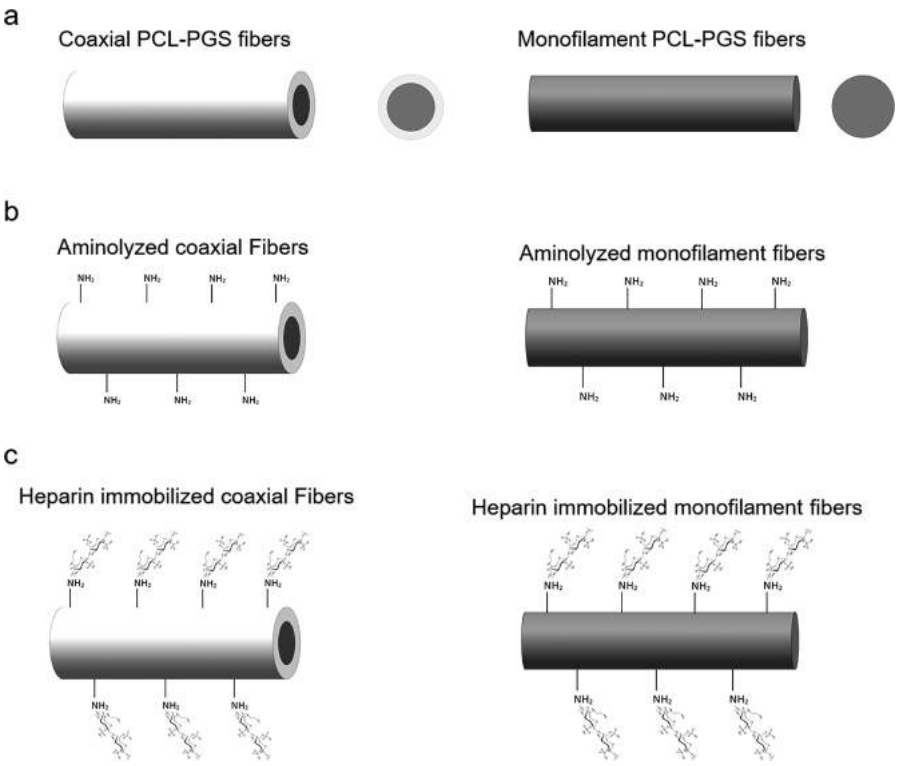

Figure 1. Drawing of types of electrospun fibers prepared for the study. NX 10 (version 10, Siemens PLM) was used. (a) Unmodified mono and coaxial PCL−PGS fibers. (b) Aminolyzed mono and coaxial PCL−PGS fibers. (c) Heparin-immobilized mono and coaxial PCL−PGS fibers.

modulus was calculated from the 0−15% strain region in the stress−strain curve. Ultimate strength (UTS) and ultimate elongation were measured from the highest peak of the stress−strain curve.

Degradation Analysis. Electrospun mats were cut into 15 mm × 5 mm × 0.2 mm rectangular strips and subjected to accelerated degradation (n = 3) by incubation in 5 mL of 1 mM NaOH solution at 37 °C for different time periods (2, 4, 8, and 12 days). After incubation at each degradation time point, the scaffolds were washed gently with phosphate-buffered saline (PBS, pH 7.4) and water and then freeze-dried under vacuum. The degraded sample was weighed (W_t), and the sample percentage mass loss calculated as $((W_o W_t)/W_o \times 100)$ on the basis of the initial mass (W_o) of each sample before incubation.

Covalent Immobilization of Heparin on PCL−PGS Mats. A previously described method was used to introduce amine groups onto 13PCL−80PGS core−shell mats.[28] Briefly, 2 cm × 2 cm × 0.2 mm mats were immersed into 10% (w/v) 1,6-hexanediamine solution prepared in isopropanol for 3 h at room temperature. Then, the aminolyzed mats were washed in deionized water for 48 h and freeze-dried under vacuum. The amine groups containing 13PCL−m-80PGS mixture-fiber mats were incubated with 300 mg of EDC and 450 mg of NHS in the presence of 10 mL of 30 mg/mL heparin solution in 10 mL of deionized water and kept at room temperature for 24 h to obtain heparin-immobilized 13PCL−m-80PGS mats. After the reaction, the fiber mat was washed with 1% Triton-X 100 aqueous solution and deionized water several times and freeze-dried under vacuum.

Procedures of Anti-IIa and Anti-Xa Assays. The 13PCL−80PGS core−shell fibers with surface-immobilized heparin were thoroughly washed with water to remove all leachable heparin prior to measuring anti-IIa and anti-Xa activities. The wells without mats were used as blank controls. Briefly, heparinized mats and nonheparinized fiber mats (~2.5 mg, n = 3) were placed in a 96-well plate. All samples and reagents were preincubated at 37 °C for 10 min. The fiber mats were mixed with reagent 1 from the BIOPHEN kits to start the assay at 37 °C. Reagents 2 and 3 and 20% acetic acid were added at 2, 4, and 5 min for anti-IIa and 6 min for anti-Xa. The absorbance was measured at 405 nm using a plate reader (Spectramax M5, MD). All samples and blanks were determined in triplicate. For calculations, the mean of blank A_{405} was subtracted from the mean of each sample.

In Vitro Cell Culture Evaluation. HUVECs were cultured in EBM-2 supplemented with growth factor kit and maintained at 37 °C and 5% CO_2. Prior to cell seeding, the scaffolds were cut into 0.5 cm × 0.5 cm × 0.2 cm and sterilized in 70% ethanol for 10 min, followed by 10 min of UV exposure. HUVEC cells were seeded at 150 000 cells per mat. The cells were allowed to attach for 1 h; then, 200 μL of fresh medium was added to each well. The WST-1 cell proliferation assay kit was used according to the manufacturer's instructions to quantitatively evaluate proliferation on seeded mats (n = 5), (Cayman, MI). Cells seeded on tissue culture plates (TCPs) served as the control. At predetermined time points (1, 3, 5, and 10 days), the medium was removed, samples washed with PBS twice to remove unattached cells, 100 μL of fresh medium was added, and then 10 μL of WST-1 solution was added and incubated for 2 h at 37 °C. The medium (100 μL) was then transferred to a 96-well plate and absorbance was measured at 450 nm. For cell attachment and cell spreading observations, seeded mats were

DOI: 10.1021/acsomega.7b00460
ACS Omega 2017, 2, 6321−6328

fixed with 70% ethanol overnight and then observed using FE-SEM at each predetermined time point.

Statistical Analysis. All data are presented as mean values ± standard deviations (SD). Statistical analysis was performed using the statistical software Origin 8.0. Significant differences between groups were measured using a *t*-test, and *p*-values less than 0.05 were considered statistically significant.

RESULTS AND DISCUSSION

Three-dimensional PCL−PGS structures have already been widely used in various tissue-engineering applications. PGS is an elastomeric polymer that has great potential in improving physical and chemical properties of scaffolds but presents challenges due to its low viscosity and the need for curing to solid polymer. PCL can provide for improved stability when added to PGS fibers. Electrospinning for the preparation of PGS and PCL composite fibers relied on both wet−wet monofilaments (Figure 1) and wet−wet coaxial electrospinning.[31] The mass fractions of PCL and PGS present in the mixture fibers and core−shell fibers are shown in Table 1.

Table 1. Weight Distribution of PCL−PGS Fibers (wt %)[a]

fibers	PCL (wt %)	PGS (wt %)
13PCL−0PGS	100	0
13PCL−40PGS	66.1	33.9
13PCL−60PGS	56.5	43.5
13PCL−80PGS	49.4	50.6
13PCL	100	0
13PCL−m-40PGS	66.1	33.9
13PCL−m-60PGS	56.5	43.5
13PCL−m-80PGS	49.4	50.6

[a]Core−shell fibers: 13PCL−0PGS, 13PCL−40PGS, 13PCL−60PGS, and 13PCL−80PGS. Mixture fibers: 13PCL (100%), 13PCL−m-40PGS, 13PCL−m-60PGS, and 13PCL−m-80PGS.

The morphology of electrospun mats composed of mixture fibers and core−shell fibers was determined using scanning electron microscopy (Figure 2). Both mixture and core−shell fibers exhibited uniform and smooth surface morphology. The anticipated fiber structure for core−shell and monofilament fibers could be observed. The cross section of core−shell fiber mats shows two distinct layers of the PCL shell and PGS core, whereas that of the mixture in the monofilament fiber mats shows only a single layer. The mean diameter of fibers was calculated using 30 different regions of each mat; the diameter varied depending on the PGS content and electrospinning technique (Figure 3a). The diameter of the mixture fibers of 13PCL alone was 520 nm, as PGS was added (13PCL−m-40PGS, 13PCL−m-60PGS, and 13PCL−m-80PGS) the diameter did not change significantly, as follows: 1.10, 1.13, and 1.10 μm, respectively. However, when examining core−shell fibers, the diameter significantly increased as PGS content increased. We found that the diameter of 13PCL−0PGS was 1.55 μm, whereas that of 13PCL−40PGS, 13PCL−60PGS, and 13PCL−80PGS was 3.09, 4.42, and 5.54 μm, respectively.

DSC was used to determine the thermal properties of the electrospun PCL−PGS mats. The relevant thermograms of the PCL−PGS fibers with different blend ratios are shown in Figure 3b. The thermograms exhibit a main melting peak at T_m = 57.8 °C, which is consistent with PCL. The melting temperature (T_m) of pure PGS was calculated to be 12.4 °C. Notably, electrospun mats of both core−shell and mixture

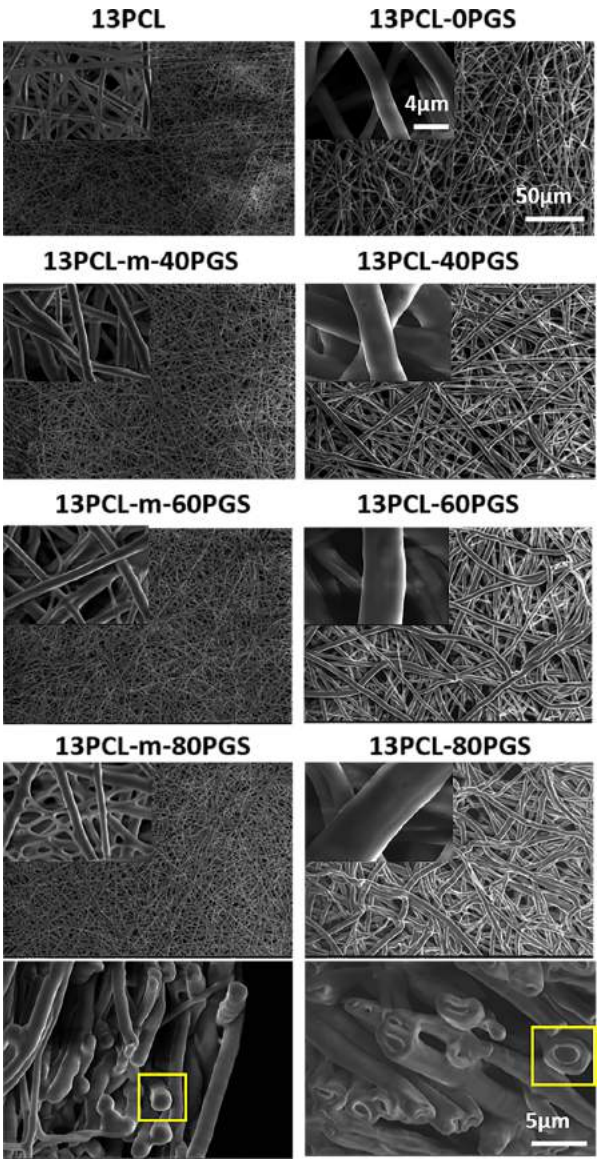

Figure 2. SEM images of mixture fibers 13PCL, 13PCL−m-40PGS, 13PCL−m-60PGS, and 13PCL−m-80PGS and core−shell fibers 13PCL−0PGS, 13PCL−40PGS, 13PCL−60PGS, and 13PCL−80PGS at 50 and 4 μm. SEM images of cross section for 13PCL−80PGS and 13PCL−m-80PGS at 5 μm.

fibers exhibited two distinct T_m, indicating presences of both PGS and PCL within the blended mats. The presence of two distinct peaks indicates that PGS and PCL are not fully miscible and phase separation might occur after the electrospinning process. On increasing the PGS blend ratio, the main melting peak shifted slightly to lower temperature. The crystallinity of the blend fibers is known to decrease with an increasing PGS/PCL blend ratio; the PGS prepolymer is fully amorphous above 35 °C. Thus, increasing the PGS content of the blend nanofiber causes a decrease in crystallinity of the fibers. It should be pointed out that low crystallinity is extremely important for good elasticity and biodegradability of a potential implant material.

DOI: 10.1021/acsomega.7b00460
ACS Omega 2017, 2, 6321−6328

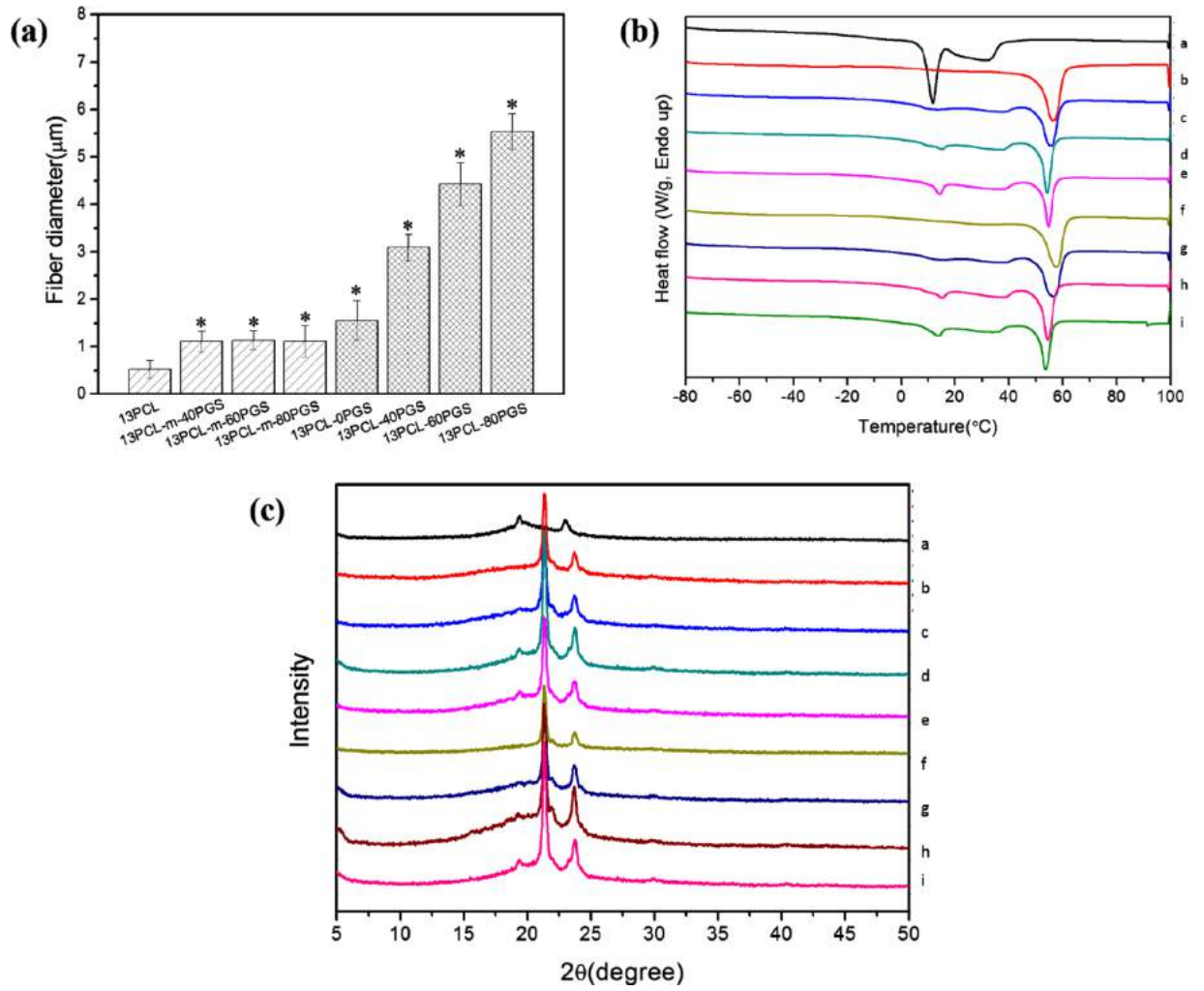

Figure 3. (a) Effect of the PCL−PGS ratio on fiber diameter. *Significance ($p < 0.05$) is based on comparison against 13PCL fiber diameter, and error bars represent the standard deviation. (b) DSC analysis of the sixth cycle of mixture fibers and core−shell fibers. (c) X-ray diffraction spectra for the mixture fibers and core−shell fibers. ((a) PGS, (b) 13PCL, (c) 13PCL−m-40PGS, (d) 13PCL−m-60PGS, (e) 13PCL−m-80PGS, (f) 13PCL−0PGS, (g) 13PCL−40PGS, (h) 13PCL−60PGS, and (i) 13PCL−80PGS).

The X-ray diffraction (XRD) pattern of the PGS prepolymer exhibits two peaks at 19 and 23 °C. Although the signals are rather weak, this is quite remarkable as the prepolymer is generally thought to be an amorphous polymer. In the case of the PCL-only fibers, two peaks are observed at 21 and 23 °C. The XRD patterns of the blend fibers are summarized in Figure 3c. The patterns exhibit three peaks, which constitute the two major peaks of the PCL spectrum and a peak at 2Θ = 19 °C, which can be assigned to the PGS portion. The presence of heparin was confirmed by its enzymatic digestion, followed by disaccharide analysis using LC/MS. Results show (Figure S1, SI section) that heparin is externally accessible in all electrospun mats. However, fibers containing PGS showed higher heparin peak intensity compared to that of fibers containing PCL alone. A standard for heparin peak intensity and compositions are included in the SI section (Figure S1 and Table S1, respectively).

Stress−strain curves for all ratios of the core−shell and mixture mats were next examined. In the mixture-fiber mats (Figure 4c), the addition of PGS resulted in a significant increase in the ultimate tensile strength (UTS). Young's modulus and extension had very little to no changes (Figure 4b,d, respectively). In contrast, the addition of PGS in the core−shell fibers resulted in a significant increase in Young's modulus extension (Figure 4b,d, respectively). Addition of PGS resulted in the decrease of UTS in the core−shell fiber mats. The stress−strain curves (Figure 4a) showed a small linear region followed by a significant deformation of the core−shell mats. Fiber morphology and diameter also play an important role in the mechanical properties of electrospun mats (Figure 2). The addition of different PGS ratios had no effect on the fiber diameter in the mixture mats; thus, Young's modulus and elongation did not change significantly. However, a different trend was observed in core−shell mats; with the PGS ratio increase, the fiber diameter increased and this resulted in an increase in Young's modulus and extension.

The degradation of mixture and core−shell mats showed linear degradation profiles for both the PCL and PCL−PGS mats (Figure 5). Under accelerated conditions for 12 days, PCL-only mats showed a 15.7% mass loss, whereas the mixture

DOI: 10.1021/acsomega.7b00460
ACS Omega 2017, 2, 6321−6328

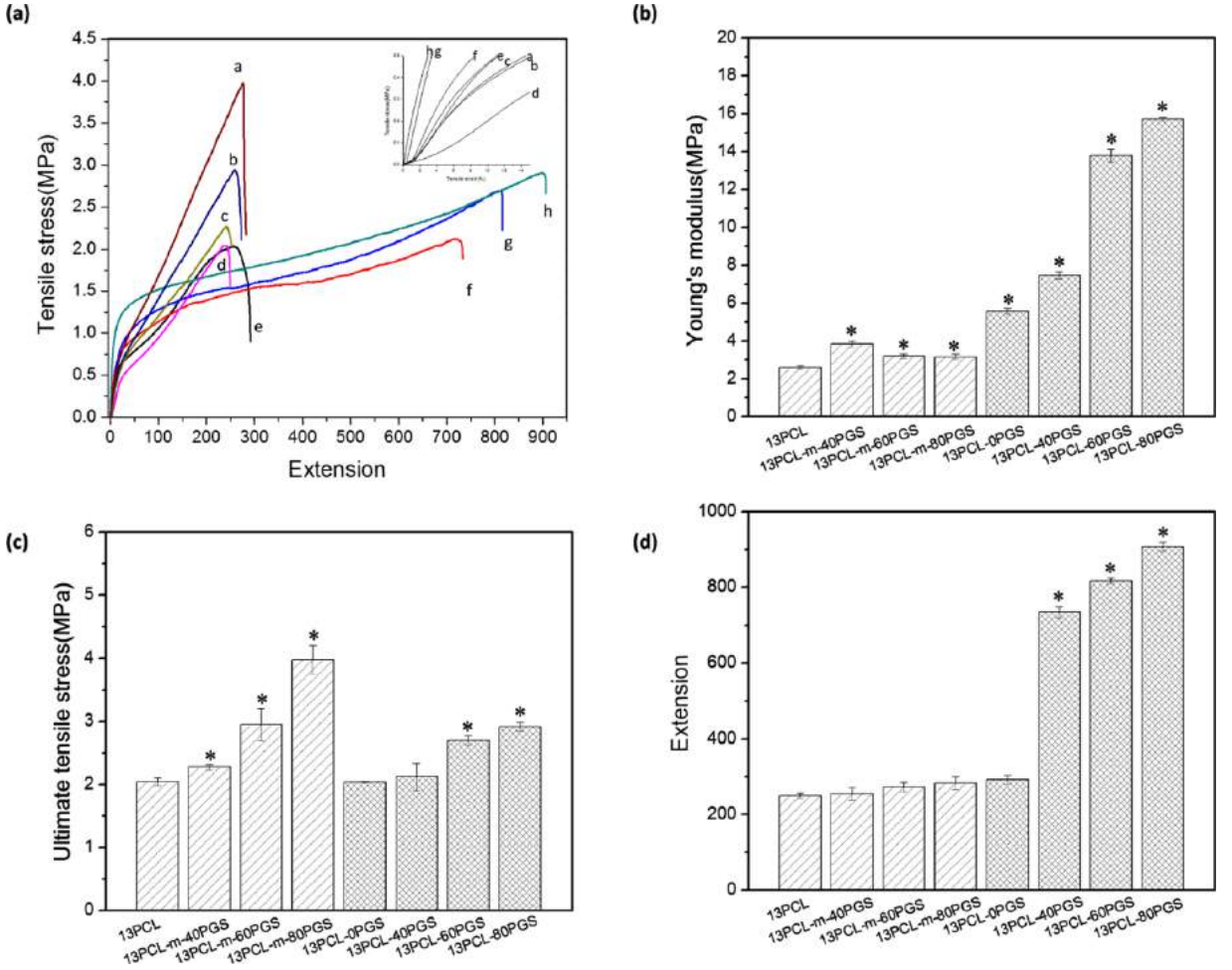

Figure 4. Mechanical properties of PCL−PGS fibers. (a) Stress−strain curves for the fibers. (b) Young's modulus, as calculated from the 0−15% linear region of the stress−strain curves. (c) Ultimate tensile stress. (d) Elongation at break. *Significance ($p < 0.05$) is based on comparison against 13PCL fiber, and error bars represent the standard deviation. ((a) 13PCL−m-80PGS, (b) 13PCL−m-60PGS, (c) 13PCL−m-40PGS, (d) 13PCL, (e) 13PCL−0PGS, (f) 13PCL−40PGS, (g) 13PCL−60PGS, and (h) 13PCL−80PGS).

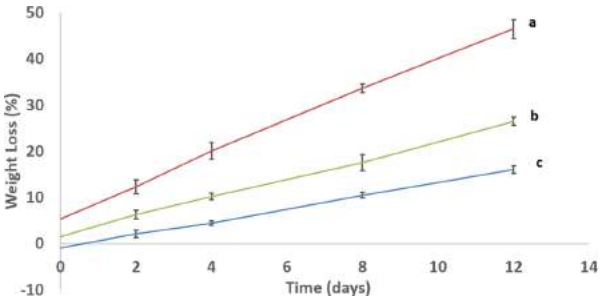

Figure 5. Accelerated in vitro degradation (mass loss, %) of (a) 13PCL−m-80PGS, (b) 13PCL−80PGS, and (c) 13PCL in 1 mM NaOH. Error bars represent the standard deviation.

mats (13PCL−m-80PGS) showed a higher degradation rate with a 45.9% mass loss and the core−shell mats (13PCL−80PGS) showed a 26.3% mass loss. Previous in vivo studies reported PGS implants of having a linear 70% mass loss within 35 days,[19] whereas PCL implants degraded slowly over more than 2 years, depending on the polymer molecular weight.[32] In an accelerated degradation study of PCL scaffolds using 5 M NaOH, a mass loss of about 15% was reported in 1 week.[33]

The anticoagulant activities of the core−shell and mixture mats, with and without surface-bound heparin, were examined using anti-Factor Xa and anti-Factor IIa assays (SI, Table S2). These amydolytic assays measure the ability of heparin on the surface of the fiber to inhibit the blood coagulation cascade proteases Factor IIa (thrombin) and Factor Xa. In this assay, if heparin is present on the fiber it binds to antithrombin, a serine protease inhibitor, which inactivates either Factor IIa or Factor Xa, preventing them to act on their amidolytic substrate to afford a colored product, *p*-nitrophenol. The core−shell 13PCL−80PGS−heparin and the mixture mat 13PCL−m-80PGS−heparin fibers, when present in the reaction media, completely inhibited color formation, confirming that active heparin anticoagulant was present on the surface of these fibers.

HUVECs were seeded on mixture and core−shell mats and cultured for 1, 3, 5, and 10 days. A quantitative analysis of cell attachment by the WST-1 assay is shown in Figure 6. All mats showed good cell metabolic activity. By day 3, the heparinized mixture and core−shell mats showed significantly higher cell activity than that of nonheparinized mats. This trend continued

DOI: 10.1021/acsomega.7b00460
ACS Omega 2017, 2, 6321−6328

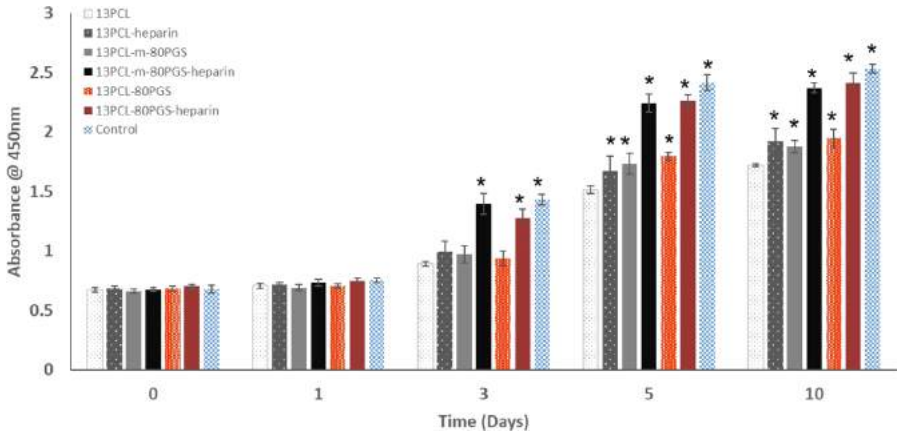

Figure 6. HUVEC proliferation on 13PCL, 13PCL−hep, 13PCL−m-80PGS, 13PCL−m-80PGS−hep, 13PCL−80PGS, and 13PCL−80PGS−hep by the WST-1 assay. *Significance ($p < 0.05$) is based on comparison against 13PCL fibers, and error bars represent the standard deviation.

through day 10. HUVEC cells grown on tissue culture plates were used as a positive control. Heparinized PCL-alone mats showed slight increase in cell activity compared to that of nonheparinized PCL-alone mats. The difference in cell activity was much more pronounced when heparinized fiber mats contained PGS. As in previous studies, the PCL−PGS mats supported the viability, attachment, proliferation, and spreading of various types of cells, including those of HUVECs. Electrospun PCL has a hydrophobic surface due to the lack of functional groups and thus does not promote cell adhesion. The addition of PGS decreases the contact angle and hydrophobicity of PCL, leading to enhanced cell attachment and spreading.[26] The heparin immobilized on the surface is capable of interacting with a great number of proteins related to cell adhesion, proliferation, or osteogenic differentiation.[34]

CONCLUSIONS

In this study, core−shell fibers of PCL (shell) and PGS (core) were prepared using wet−wet coaxial electrospinning. Then, the heparin was immobilized on the surface of the PCL/PGS scaffold. Fabricated scaffolds were evaluated for their chemical, mechanical, and biological properties. The core−shell structure of PCL with PGS allows controlled degradation of the scaffold. Slowly degrading PCL will provide structural integrity and mechanical support, whereas the fast degrading PGS component will increase the elasticity, maintaining the mechanical properties of the tissue-engineered construct. The PGS−PCL scaffolds showed tunable mechanical properties so that Young's modulus changed from 5.56 to 15.7 MPa, ultimate tensile stress changed from 2.04 to 2.91 MPa, and elongation changed from 291 to 907%. The addition of PGS and the grafting of heparin improved cell attachment and proliferation of human umbilical vein endothelial cells (HUVECs). The scaffolds provide the potential applications in tissue engineering.

ASSOCIATED CONTENT

Supporting Information

The Supporting Information is available free of charge on the ACS Publications website at DOI: 10.1021/acsomega.7b00460.

LC−MS analysis of heparin in 13PCL, 13PCL−m-80PGS, and 13PCL−80PGS fibers (SI, Figure S1); analysis of the standard sample (SI, Table S1); anticoagulant activity of 13PCL−hep, 13PCL−m-80PGS−hep, and 13PCL−80PGS−hep (SI, Table S2) (PDF)

AUTHOR INFORMATION

Corresponding Authors

*E-mail: mikaep@rpi.edu. Tel: (518) 276-6749 (P.E.M.).
*E-mail: linhar@rpi.edu. Tel: (518) 276-3404 (R.J.L.).

ORCID

Paiyz E. Mikael: 0000-0003-4679-9770
Fuming Zhang: 0000-0003-2803-3704
Robert J. Linhardt: 0000-0003-2219-5833

Author Contributions

The study was performed by L.H., X.Z., and L.L. The article was written by L.H., P.E.M., and R.J.L.

Notes

The authors declare no competing financial interest.

ACKNOWLEDGMENTS

The authors acknowledge the helpful guidance of the manager of the electron microscopy laboratory, Raymond P. Dove III Esq., for SEM and TEM assistance and the analytical core facility director, Dr. Joel Morgan, for XRD and TGA assistance. We also thank Charles Willard, an undergraduate research student at RPI, for preparing Figure [1,].

REFERENCES

(1) Langer, R.; Vacanti, J. P. Tissue Engineering. *Science* **1993**, *260*, 920−926.

(2) Nair, L. S.; Laurencin, C. T. Polymers as Biomaterials for Tissue Engineering and Controlled Drug Delivery. In *Tissue Engineering I*; Advances in Biochemical Engineering/Biotechnology, 2006; Vol. *102*, pp 47−90.

(3) Karande, T.; Kaufmann, J. J. M.; Agrawal, C. *Function and Requirement of Synthetic Scaffolds in Tissue Engineering*, 2nd ed.; CRC Press: Boca Raton, 2008.

(4) Igwe, J.; Amini, A.; Mikael, P.; Laurencin, C.; Nukavarapu, S. Nanostructured Scaffolds for Bone Tissue Engineering. In *Active Implants and Scaffolds for Tissue Regeneration*; Zilberman, M., Ed.; Springer, 2011; Vol. *8*, pp 169−192.

(5) Viswanathan, G.; Murugesan, S.; Pushparaj, V.; Nalamasu, O.; Ajayan, P. M.; Linhardt, R. J. Preparation of biopolymer fibers by electrospinning from room temperature ionic liquids. *Biomacromolecules* **2006**, *7*, 415−418.

DOI: 10.1021/acsomega.7b00460
ACS Omega 2017, 2, 6321−6328

(6) Meli, L.; Miao, J. J.; Dordick, J. S.; Linhardt, R. J. Electrospinning from room temperature ionic liquids for biopolymer fiber formation. *Green Chem.* **2010**, *12*, 1883−1892.
(7) Miao, J.; Miyauchi, M.; Simmons, T. J.; Dordick, J. S.; Linhardt, R. J. Electrospinning of Nanomaterials and Applications in Electronic Components and Devices. *J. Nanosci. Nanotechnol.* **2010**, *10*, 5507−5519.
(8) Baker, S.; Sigley, J.; Helms, C. C.; Stitzel, J.; Berry, J.; Bonin, K.; Guthold, M. The mechanical properties of dry, electrospun fibrinogen fibers. *Mater. Sci. Eng., C* **2012**, *32*, 215−221.
(9) Maeda, N.; Miao, J.; Simmons, T. J.; Dordick, J. S.; Linhardt, R. J. Composite polysaccharide fibers prepared by electrospinning and coating. *Carbohydr. Polym.* **2014**, *102*, 950−955.
(10) Sperling, L. E.; Reis, K. P.; Pranke, P.; Wendorff, J. H. Advantages and challenges offered by biofunctional core−shell fiber systems for tissue engineering and drug delivery. *Drug Discovery Today* **2016**, *21*, 1243−1256.
(11) Kostakova, E.; Seps, M.; Pokorny, P.; Lukas, D. Study of polycaprolactone wet electrospinning process. *eXPRESS Polym. Lett.* **2014**, *8*, 554−564.
(12) Zheng, Y.; Monty, J.; Linhardt, R. J. Polysaccharide-based nanocomposites and their applications. *Carbohydr. Res.* **2015**, *405*, 23−32.
(13) Wang, Y.; Ameer, G. A.; Sheppard, B. J.; Langer, R. A tough biodegradable elastomer. *Nat. Biotechnol.* **2002**, *20*, 602−606.
(14) Fidkowski, C.; Kaazempur-Mofrad, M. R.; Borenstein, J.; Vacanti, J. P.; Langer, R.; Wang, Y. D. Endothelialized microvasculature based on a biodegradable elastomer. *Tissue Eng.* **2005**, *11*, 302−309.
(15) Radisic, M.; Park, H.; Martens, T. P.; Salazar-Lazaro, J. E.; Geng, W. L.; Wang, Y. D.; Langer, R.; Freed, L. E.; Vunjak-Novakovic, G. Pre-treatment of synthetic elastomeric scaffolds by cardiac fibroblasts improves engineered heart tissue. *J. Biomed. Mater. Res., Part A* **2008**, *86*, 713−724.
(16) Chen, Q. Z.; Bismarck, A.; Hansen, U.; Junaid, S.; Tran, M. Q.; Harding, S. E.; Ali, N. N.; Boccaccini, A. R. Characterisation of a soft elastomer poly(glycerol sebacate) designed to match the mechanical properties of myocardial tissue. *Biomaterials* **2008**, *29*, 47−57.
(17) Engelmayr, G. C., Jr.; Cheng, M. Y.; Bettinger, C. J.; Borenstein, J. T.; Langer, R.; Freed, L. E. Accordion-like honeycombs for tissue engineering of cardiac anisotropy. *Nat. Mater.* **2008**, *7*, 1003−1010.
(18) Sundback, C. A.; Shyu, J. Y.; Wang, Y. D.; Faquin, W. C.; Langer, R. S.; Vacanti, J. P.; Hadlock, T. A. Biocompatibility analysis of poly(glycerol sebacate) as a nerve guide material. *Biomaterials* **2005**, *26*, 5454−5464.
(19) Wang, Y.; Kim, Y. M.; Langer, R. In vivo degradation characteristics of poly(glycerol sebacate). *J. Biomed. Mater. Res., Part A* **2003**, *66*, 192−197.
(20) Ifkovits, J. L.; Devlin, J. J.; Eng, G.; Martens, T. P.; Vunjak-Novakovic, G.; Burdick, J. A. Biodegradable Fibrous Scaffolds with Tunable Properties Formed from Photo-Cross-Linkable Poly(glycerol sebacate). *ACS Appl. Mater. Interfaces* **2009**, *1*, 1878−1886.
(21) Yi, F.; LaVan, D. A. Poly(glycerol sebacate) nanofiber scaffolds by core/shell electrospinning. *Macromol. Biosci.* **2008**, *8*, 803−806.
(22) Couet, F.; Rajan, N.; Mantovani, D. Macromolecular biomaterials for scaffold-based vascular tissue engineering. *Macromol. Biosci.* **2007**, *7*, 701−718.
(23) Lee, S. J.; Liu, J.; Oh, S. H.; Soker, S.; Atala, A.; Yoo, J. J. Development of a composite vascular scaffolding system that withstands physiological vascular conditions. *Biomaterials* **2008**, *29*, 2891−2898.
(24) de Valence, S.; Tille, J. C.; Mugnai, D.; Mrowczynski, W.; Gurny, R.; Moller, M.; Walpoth, B. H. Long term performance of polycaprolactone vascular grafts in a rat abdominal aorta replacement model. *Biomaterials* **2012**, *33*, 38−47.
(25) Dash, T. K.; Konkimalla, V. B. Poly-epsilon-caprolactone based formulations for drug delivery and tissue engineering: A review. *J. Controlled Release* **2012**, *158*, 15−33.
(26) Sant, S.; Hwang, C. M.; Lee, S. H.; Khademhosseini, A. Hybrid PGS-PCL microfibrous scaffolds with improved mechanical and biological properties. *J. Tissue Eng. Regener. Med.* **2011**, *5*, 283−291.
(27) Tallawi, M.; Dippold, D.; Rai, R.; D'Atri, D.; Roether, J. A.; Schubert, D. W.; Rosellini, E.; Engel, F. B.; Boccaccini, A. R. Novel PGS/PCL electrospun fiber mats with patterned topographical features for cardiac patch applications. *Mater. Sci. Eng., C* **2016**, *69*, 569−576.
(28) Murugesan, S.; Xie, J.; Linhardt, R. J. Immobilization of heparin: Approaches and applications. *Curr. Top. Med. Chem.* **2008**, *8*, 80−100.
(29) Dimitrievska, S.; Cai, C.; Weyers, A.; Balestrini, J. L.; Lin, T.; Sundaram, S.; Hatachi, G.; Spiegel, D. A.; Kyriakides, T. R.; Miao, J. J.; Li, G. Y.; Niklason, L. E.; Linhardt, R. J. Click-coated, heparinized, decellularized vascular grafts. *Acta Biomater.* **2015**, *13*, 177−187.
(30) Rai, R.; Tallawi, M.; Frati, C.; Falco, A.; Gervasi, A.; Quaini, F.; Roether, J. A.; Hochburger, T.; Schubert, D. W.; Seik, L.; Barbani, N.; Lazzeri, L.; Rosellini, E.; Boccaccini, A. R. Bioactive Electrospun Fibers of Poly(glycerol sebacate) and Poly(e-caprolactone) for Cardiac Patch Application. *Adv. Healthcare Mater.* **2015**, *4*, 2012−2025.
(31) Hou, L.; Udangawa, W. M. R. N.; Pochiraju, A.; Dong, W.; Zheng, Y.; Linhardt, R. J.; Simmons, T. J. Synthesis of Heparin-Immobilized, Magnetically Addressable Cellulose Nanofibers for Biomedical Applications. *ACS Biomater. Sci. Eng.* **2016**, *2*, 1905−1913.
(32) Sun, H.; Mei, L.; Song, C. X.; Cui, X. M.; Wang, P. Y. The in vivo degradation, absorption and excretion of PCL-based implant. *Biomaterials* **2006**, *27*, 1735−1740.
(33) Lam, C. X. F.; Savalani, M. M.; Teoh, S. H.; Hutmacher, D. W. Dynamics of in vitro polymer degradation of polycaprolactone-based scaffolds: accelerated versus simulated physiological conditions. *Biomed. Mater.* **2008**, *3*, No. 034108.
(34) Benoit, D. S. W.; Durney, A. R.; Anseth, K. S. The effect of heparin-functionalized PEG hydrogels on three-dimensional human mesenchymal stem cell osteogenic differentiation. *Biomaterials* **2007**, *28*, 66−77.

DOI: 10.1021/acsomega.7b00460
ACS Omega 2017, 2, 6321−6328